Low resistivity Ga-doped ZnO thin films of less than 100 nm thickness prepared by ion plating with direct current arc discharge

doi: 10.1063/1.2767213

Low resistivity Ga-doped ZnO thin films of less than 100 nm thickness prepared by ion plating with direct current arc discharge

Takahiro Yamada,[a] Aki Miyake, Seiichi Kishimoto, Hisao Makino, Naoki Yamamoto, and Tetsuya Yamamoto
Kochi University of Technology, 185, Miyanokuchi, Tosayamada, Kami, Kochi 782-8502, Japan

(Received 21 May 2007; accepted 9 July 2007; published online 1 August 2007)

Low resistivity Ga-doped ZnO films were prepared on a glass substrate by ion plating with direct current arc discharge. Thickness dependent changes in the electrical properties of the films are reported, focusing on the thin films of less than 100 nm thickness. Structural analyses showed that the thinnest film of 30 nm thickness consists of well-oriented columnar grains normal to the substrate, and the resistivity was as low as 4.4×10^{-4} Ω cm. The changes in lattice strain and *c*-axis fluctuation with the growth of grains are also shown to be associated with the electrical properties. © *2007 American Institute of Physics*. [DOI: 10.1063/1.2767213]

In this work, we report the fabrication of low resistivity and preferentially *c*-axis oriented Ga-doped ZnO (GZO) films with thickness of less than 100 nm. Much effort has been devoted to the development of an alternative to indium-based transparent electrodes because of the scarcity of its principal component, indium. ZnO is one candidate material for its replacement.[1] However, for practical use, ZnO films have some problems requiring a solution, e.g., an electrical stability for heat and moisture resistances, etc.[2] One of them is the dependence of resistivity on the thickness of ZnO films. Here, in the case of indium tin oxide (ITO) electrodes used in various displays, the thickness ranges from 15 to 450 nm,[3,4] It is practically determined in terms of etching property, the influence of light interference and a process time and costs spent in display fabrication, etc. Even for such thickness of less than 100 nm, the low resistivity of ITO is maintained. On the other hand, in the case of ZnO films, it is well known that the crystalline qualities of ZnO films prepared on glass or organic substrates strongly depend on their thickness, and consequently, the resistivity increases with decreasing film thickness.[5,6] Thus, the film thickness is one of significant parameters determining the electrical properties of ZnO films. However, there have been few reports on the thickness dependent changes in the properties of ZnO films with a thickness of less than 100 nm, although those in ITO films have been reported by several authors.[3] In this work, we succeeded in obtaining a resistivity of as low as 4.4×10^{-4} Ω cm in GZO film with a thickness of 30 nm. The discussion will focus on the growth of GZO film consisting of columnar grains and the correlation between the electrical properties and the orientation of GZO films with thicknesses of less than 100 nm.

GZO films were deposited on an alkali-free glass substrate at 473 K using an ion-plating system with a direct current (dc) arc discharge using a pressure-gradient-type plasma gun.[7] A series of GZO films with thicknesses range from 30 to 98±3 nm were prepared by changing the deposition time. The base pressure in the chamber was about 2.0×10^{-5} Pa. After evacuation of the chamber, argon and oxygen gases were introduced at the gas flow rates of 140 and 8 SCCM (SSCM denotes cubic centimeter per minute at STP), respectively, and the deposition pressure was 2.2×10^{-1} Pa. A sintered ZnO ceramic target containing 4 wt % Ga_2O_3 powder was used as a source material (99.99% purity, Hakusui Tech.). The applied-discharge current between the target and the plasma gun was automatically controlled to be 140 A. These conditions were set to obtain the minimum resistivity of the GZO film.

The thickness of the film was measured using a surface profilometer (Alfa-Step, IQ). The electrical properties of the films were characterized by Hall effect measurements in the van der Pauw configuration (Accent, HL5500PC) at room temperature. The *c*-axis orientation, its fluctuation and the lattice parameters of the films were characterized by high-resolution x-ray diffraction (XRD) Rigaku, ATX-G system) analysis using Cu $K\alpha$ radiation ($\lambda=1.5406$ Å). Direct observation of the film with a thickness of 30 nm was carried out using a cross-sectional transmission electron microscope (TEM) (JEOL, JEM-2100F).

Polycrystalline ZnO thick films deposited on amorphous substrates generally consist of columnar grains grown with the orientation of the [0002] *c*-axis direction normal to the substrates. The orientation of the grains has been often investigated as an index representing the crystalline quality of the film. In the case of thinner ZnO films with a thickness of less than 100 nm, the orientation is partially random,[5] which is related to the formation of grains in the initial stage of film deposition. The random orientation strongly influences the electrical properties of the film. Thus, for the thinnest GZO film with a thickness of 30 nm, the grain structure was investigated by XRD measurements and direct cross-sectional TEM observations. Figure 1 shows a XRD θ-2θ scan profile of the film. The diffraction intensity on the vertical axis is expressed in a logarithmic scale. In Fig. 1, only two diffraction peaks from ZnO (0002) and (0004) planes can be recognized. The XRD pattern shows that the film is polycrystalline with a wurtzite-type hexagonal structure and has a preferential orientation of *c* axis normal to the substrate. This orientation can also be observed from a cross-sectional TEM image of the film, as shown in Fig. 2. It is obvious that the film is a well-aligned polycrystalline film. As indicated by a broken line, a clear columnar structure with a grain size of about 15 nm, where no crystallites are overgrown, is observed, and most of the columnar grains are grown normal to

[a]Electronic mail: yamada.takahiro@kochi-tech.ac.jp

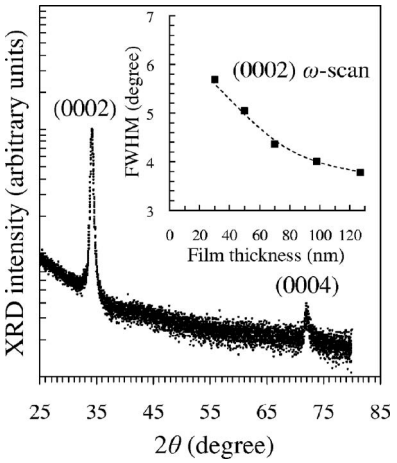

FIG. 1. Typical XRD θ-2θ scan profile of the GZO film with a thickness of 30 nm. The diffraction intensity on the vertical axis is expressed in a logarithmic scale. The inset shows the full width at half maximum of (0002) ω-scan rocking curve as a function of film thickness below 98 nm.

the substrate. No other phases such as Ga_2O_3 or amorphous ZnO are recognized at the grains and the grain boundaries. This observation is consistent with the result of the XRD pattern shown in Fig. 1. Moreover, it has been observed that (0002) lattice fringes along the substrate plane immediately appear at the interface between the substrate and the film; a similar result has been also reported in the case of relatively thick films.[8] These results provide us with strong evidence that, even at a thickness of only 30 nm, the film is composed of the equiaxed columnar grains grown from the initial stage of film deposition.

This crystallization from the interface is attributed to a high-density plasma exposure to the surface. In our deposition, the deposition rate is 3.0 nm/s, which is higher compared with that of conventional sputtering (1.1 nm/s in Ref. 5). This is due to the high-density plasma flux exposure of sublimated and ionized target elements to the substrate, where no substrate bias is applied. The degree of surface damage due to the plasma bombardment is also low. Thus, the surface is strongly activated with various plasma-surface interactions such as thermal heating, selective etching, surface diffusion, etc. These effects increase the nucleation density and promote the grain growth along the lowest surface energy plane, determining the preferential c-axis orientation

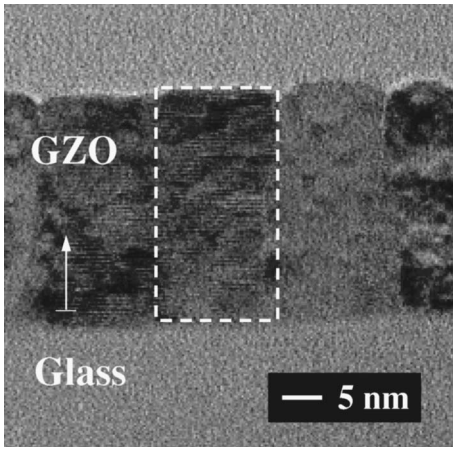

FIG. 2. Cross-sectional TEM image of the GZO film with a thickness of 30 nm. A single column is indicated by a broken line.

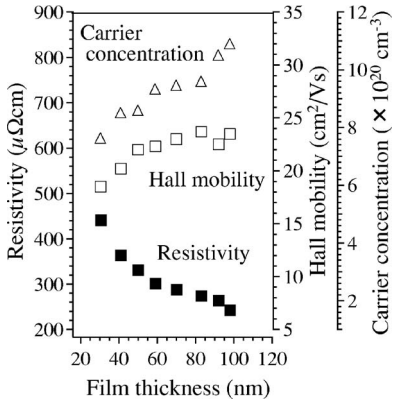

FIG. 3. Resistivity, carrier concentration, and Hall mobility of GZO films as a function of film thickness in the range from 30 to 98 nm.

of the films.[9,10] Consequently, as observed in Fig. 2, the equiaxed columnar grains will be grown from the interface.

Here, we will turn to the discussion about the thickness dependence. Figure 3 shows the resistivity, carrier concentration, and Hall mobility of GZO films as a function of film thickness in the range from 30 to 98 nm. In Fig. 3, the resistivity decreased with increasing film thickness, resulting from increases in both the carrier concentration and the Hall mobility. For the film with a thickness of 98 nm, a resistivity of as low as 2.4×10^{-4} Ω cm was obtained at a carrier concentration of 1.1×10^{21} cm^{-3} and a Hall mobility of 23.5 cm^2/V s. From a comparison with Ref. 11, this value was found to be close to that, 1.5×10^{-4} Ω cm, of an ITO film with almost the same thickness (100 nm), where the ITO film is prepared in a similar manner to our GZO films except for the use of dc magnetron sputtering. Moreover, even for the thinnest film with a thickness of 30 nm, the resistivity was as low as 4.4×10^{-4} Ω cm. These low resistivities for the thin films indicate that a high quality GZO film is formed from the early stage of film deposition. This is correlated with the grain growth at the interface. Here, it was confirmed from secondary ion mass spectroscopy analysis that the gallium concentration in the GZO films is uniformly distributed from the surface to the interface, and the average concentration remains almost constant at 1.5×10^{21} cm^{-3}, independent of the film thickness.

In the growth of GZO films from the early stage, various phenomena corresponding to the improvement of crystalline quality simultaneously occur. We have revealed that, with increasing film thickness in this range, the film crystallinity is improved, where the full width at half maximum (FWHM) of ZnO (0002) XRD θ-2θ peak profile decreases from 0.48° to 0.31°, and the crystallite size increases from 18 to 26 nm.[12] Moreover, the thickness dependent changes in a lattice strain were investigated. Figure 4 shows the lattice parameters of the a and c axes of the GZO films as a function of film thickness. These parameters are determined by the analysis of in-plane and out-of-plane XRD peak profiles. The volume of the crystallographic unit cell, which is calculated with the lattice parameters, is also shown. In Fig. 4, the lattice parameters of the a and c axes gradually increase and decrease with increasing film thickness, respectively. The calculated volume remains almost constant with increasing film thickness, even when the lattice parameters rapidly change in the range of thinner thickness. Accordingly, the variations in the lattice parameters can be inter-

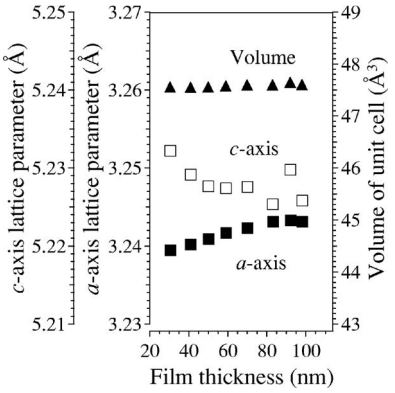

FIG. 4. Lattice parameters of *a* and *c* axes in GZO films as a function of film thickness below 98 nm. These parameters are determined by the analysis of in-plane and out-of-plane XRD peak profiles. The volume of the crystallographic unit cell, calculated with the lattice parameters, is also shown.

preted as the relaxation of compressed lattice strain in the *a*-axis direction parallel to the substrate plane. This result suggests that the films are deposited through islandlike three-dimensional grain growth. Moreover, the relaxation of the strain enhances the *c*-axis orientation. The FWHM of (0002) XRD ω-scan rocking curve for the GZO films was also investigated. As shown in the inset of Fig. 1, the FWHM decreased from 5.7° to 3.8° with increasing film thickness. This means that the degree of *c*-axis fluctuation between grains gradually decreases.

The equiaxed columnar structures of Fig. 2 are formed by the grain growth in the initial stage of film deposition. Thus, it is suggested that GZO films with few defects are already formed in the near interface. Moreover, such phenomena which occur with the film growth further enhance the crystalline quality, leading to the increase in both carrier concentration and Hall mobility. The improvement of the crystallinity leads to fewer intrinsic defects, which act as scattering and trapping centers of carrier, in the grain. The increase in the crystallite size weakens boundary scattering and increases carrier lifetime. Moreover, the relaxation of the compressed strain and the improvement of the *c*-axis fluctuation could also decrease intrinsic defects. It has been reported by Birkholz *et al.* that the crystallographic anisotropy between grains influences the mobility of carriers across the grain boundaries.[5] Such an effect may also contribute to the increase in the Hall mobility.

In summary, thickness dependent changes in the electrical properties of GZO films are reported, focusing on the thin films of less than 100 nm thickness. For the thinnest film with a thickness of 30 nm, the resistivity is as low as 4.4×10^{-4} Ω cm, where the resistivity decreases with increasing film thickness. Structural analyses indicate that the film has a preferential orientation of *c* axis normal to the substrate and is a well-aligned polycrystalline film consisting of clear columnar grains grown from the substrate plane. The *c*-axis orientation is further enhanced with increasing film thickness, simultaneously causing the relaxation of compressed lattice strain in the *a*-axis direction parallel to the substrate plane. This is argued as a factor causing the dependences of the electrical properties on film thickness.

The financial support from the collaboration of Regional Entities for the Advancement of Technological Excellence of the Japan Science and Technology Agency is gratefully acknowledged.

[1] H. Agura, A. Suzuki, T. Matsushita, T. Aoki, and M. Okuda, Thin Solid Films **445**, 263 (2003).
[2] O. Nakagawa, Y. Kishimoto, H. Seto, Y. Koshido, Y. Yoshino, and T. Makino, Appl. Phys. Lett. **89**, 091904 (2006).
[3] H. C. Lee and O. O. Park, Vacuum **80**, 880 (2006).
[4] T. Minami, T. Miyata, Y. Ohtani, and T. Kuboi, Phys. Status. Solidi Rapid Res. Lett. **1**, R31 (2007).
[5] M. Birkholz, B. Selle, F. Fenske, and W. Fuhs, Phys. Rev. B **68**, 205414 (2003).
[6] H. Hirasawa, M. Yoshida, S. Nakamura, Y. Suzuki, S. Okada, and K. Kondo, Sol. Energy Mater. Sol. Cells **67**, 231 (2001).
[7] J. Uramoto, J. Vac. Soc. Jpn. **25**, 660 (1982).
[8] X. Jiang, C. L. Jia, and B. Szyszka, Appl. Phys. Lett. **80**, 3090 (2002).
[9] Y. Kajikawa, S. Noda, and H. Komiyama, J. Vac. Sci. Technol. A **21**, 1943 (2003).
[10] Y. Kajikawa, J. Cryst. Growth **289**, 387 (2006).
[11] U. Betz, M. K. Olsson, J. Marthy, M. F. Escolá, and F. Atamny, Surf. Coat. Technol. **200**, 5751 (2006).
[12] T. Yamada, S. Kishimoto, H. Makino, N. Kuroiwa, and T. Yamamoto, *Proceedings of the Sixth International Conference on Coatings on Glass and Plastics* (ICCG, Dresden, 2006), p. 335.